

# Forming limit curves of ultra-thin sheet metal for high-speed Nakajima test

Ying Zhang (✉ [zhangying@sdjzu.edu.cn](mailto:zhangying@sdjzu.edu.cn))

Shandong Jianzhu University

Chen Yu Xie

Shandong Jianzhu University

Zheng Jun Yuan

Shandong Jianzhu University

Xiu Jia Tang

Shandong Jianzhu University

Guoqing Zhang

Shandong Energy Group

---

## Research Article

**Keywords:** High-speed forming, Microforming, Forming limit curves

**Posted Date:** March 17th, 2022

**DOI:** <https://doi.org/10.21203/rs.3.rs-1304459/v1>

**License:**  This work is licensed under a Creative Commons Attribution 4.0 International License.

[Read Full License](#)

---

# Abstract

This paper is concerned with Nakajima test and forming limit curve (FLC) of stainless 304 ultra-thin sheet metal in relation to the strain rate effect. The mechanical properties related to the micro structure of specimens are studied based on quasi static tension test. The forming limit curves are constructed by Nakajima tests with two different strain rates, quasi-static and high speed strain rate. Compared with the quasi-static FLC, the high speed FLC of the 304 ultra-thin metal sheet for all specimens with different thickness is lower through the entire region. The results confirm that the strain rates have a noticeably influence on the formability of ultra-thin sheet metal. The deformation and fracture behavior for high speed forming is discussed based on the previous study. The forming limit curves should be considered in the design in high speed ultra-thin sheet metal forming processes.

## Introduction

The rapid development of micro-electronics industry has led to the tremendous demands of parts with dimensions in submillimeter range. Metal forming through plastic deformation is one of the most efficient and economical manufacturing process for producing products at micro scales. To assist manufacturers for increase in parts productivity and reduction in the processing time, researchers are actively engaged in improving the forming speed. High strain rate forming is gradually applied to the forming techniques.

Since Clark and Wood(1950) firstly reported the strain rate sensitivity of certain materials in terms of an increased forming limit under high strain rate forming, high-speed forming process appears as a suitable approach to extend the forming limits[1]. Many researchers have investigated the effect of strain rate under high-speed deformation on the sheet metal formability. Balanethiram and Daehn(1992) presented an increase of forming limit in the biaxial stretch region for steel[2]. Similar high strain rate increase forming limits results had been reported by Balanethiram and Dehn(1994)[3]. Hu(2014) indicated that strain rate could influence the forming limits of TRIP450/800[4]. Kim(2011) presented the high-speed FLC of CQ was higher than the static in the tension region but lower than the static result in biaxial stretch forming region[5]. Kiliclar(2014) investigated the forming limits for aluminium alloy sheet metal with the specimen thickness of 1mm, results showed increased formability at a punch speed of 21m/s than at a punch 1mm/s[6]. However, it had been shown that an actual extension of forming limits requires a careful adjustment of the parameters(Taebi,2012)[7]. Nathalie(2017) presented the quasi static and dynamic Nakajima tests of the tested DC01. In the area of biaxial stretching, the forming limit in quasi-static was much higher than the dynamic case, while the result was contrary in the area of uniaxial stretching. As reviews above, the effects of high strain rates to the forming process mainly focus on dimension under meter scales. Up to now, no satisfactory test methods to determine forming limit at high strain rates according to industrial level.

As the dimensions of parts scale down from macro to micro level, the traditional forming theories are rendered inefficient in the analysis of micro deformation behaviors due to the so-called size effect[8]. Both the experiment and numerical simulations shows a significant influence of the size effect on the

cracking character as the dimensions down to micro level. The forming limit curve shifts downwards with the decreasing thickness grain size ratio[9, 10]. However, the deformation properties of ultra-thin sheet metal at high strain rate are different from that at quasi static strain rate. Malik(2019) presented dynamic compression under high strain rate is more uniform in comparison of quasi-static test[11]. Zhu(2021) indicated the fracture mode of pure titanium foil exhibits a sensitivity to high strain rate, which transform from mixed fracture of ductile fracture and cleavage fracture to thorough ductile fracture when tension strain rate from quasi-static to high strain rate[12]. Investigation on the size effects at high strain rate is still in discussion.

For this study, stainless 304 ultra-thin sheet metal with different kinds of thickness is selected for the purpose of investigation how the strain rate affects the forming limit. First, uniaxial tensile test is conducted to see the mechanical properties for the thickness in submillimeter range and the size effect. Secondly, a high speed crash testing device is designed so that we could abstain the forming limit curves under high speed Nakajima test. Finally the forming limit curves under high speed forming and quasi-static forming are compared and studied.

## **Mechanical Properties And Microstructure Analysis**

### **1.1. Tension test**

Recrystallized stainless 304 with the thicknesses of 30  $\mu\text{m}$ , 60 $\mu\text{m}$ , 100 $\mu\text{m}$  is used in the study. The chemical composition is listed in Tab.1. The first subject in investigations is determination of the mechanical properties for the ultra-thin specimens. For this purpose the tensile test is employed, focus on the stress, the strain and the ductility. The test specimens are prepared in the loading directions: the rolling direction(RD), the diagonal direction(DD), and the transverse direction(TD). Fig. 1 shows a tensile specimen with the parallel region 30mm, the width of 10 and the fillet radius of 30. Tensile test procedure is conducted with the testing machine MTS at tensile speed 0.08mm/s.

The strain hardening coefficient( $n$ ), the ratio of yield stress(YS) to ultimate tensile strength(UTS), the elongation at fracture(EI) and the anisotropy Coefficient( $r$ ) are obtained from the true stress-strain curves as shown in Tab.2. The tangent modulus is fitted by the least square method for the linear change of material in plastic stage. The test results indicate the strong influence of the size of specimen. The YS/UTS value approximates the value of 0.5 for both cases. The specimen with thickness of 10 $\mu\text{m}$  shows higher hardening coefficient than the other ones. The specimen with thickness of 100 $\mu\text{m}$  shows the highest elongation at fracture for about 200% more than the other ones, which implies that it has the best formability performance compared to others. The anisotropy is observed from both cases. However, the anisotropy  $r$  does not seem to change significantly with the specimen dimensions.

### **1.2. Metallographic experiment and discusson**

For characterization of ultra-thin sheet metal, a micro-structural investigation is performed with optical microscopy. For metallography purpose, specimens are polished with colloidal silica before etching with

solution (30mL concentrated hydrochloric acid [HCl], 10mL concentrated nitric acid [HNO<sub>3</sub>]).

The microstructures of the plane for the specimens are shown in Fig. 2, the average grain size  $d$  of 20 $\mu$ m for different thickness of the specimens. The deformation character is significantly related to the micro structure of specimens. With the different grain numbers through the thickness section, the mechanical properties show a certain size effect. Many previous researches have reported that when the ratio of specimen thickness to grain size decreases to a critical value, not only the flow stress and ductility of the material but also the fracture mode and the surface roughness of the deformed samples will change a lot. For the thickness of 30 $\mu$ m specimen, there are almost one or two grains across the section, the flow stress shows the tendency "The thinner the weaker". For the thickness of 60 $\mu$ m specimen and 100 $\mu$ m specimen, there are several grains across the section. There are more grains for the thickness of 60 $\mu$ m specimen than the thickness of 100 $\mu$ m specimen with thickness effect "thinner is stronger". Geiger and Engel proposed the widely accepted surface layer model that can explained "The thinner the weaker". The grains in deformation zone are divided into surface grains and internal grains and it is considered that surface grains have lower flow stress than internal grains because of enduring less restrictions and lower dislocations pile up ability in this model.

Table.1 Chemical composition of 304

C	Si	Mn	P	S	Cr	Ni
0.05	0.32	1.1	0.026	0.002	18.01	8.02

Tab.2 Mechanical properties

Thickness ( $\mu$ m)	Loading direction	YS(MPa)	UTS(MPa)	El(%)	r	n
30	RD	343	700	5.07	1.021	0.293
	DD	320	680	5.01	1.015	0.287
	TD	321	682	4.98	1.016	0.289
60	RD	750	1214	5.4	1.622	0.122
	DD	720	1198	5.3	1.619	0.119
	TD	701	1180	5.1	1.612	0.117
100	RD	450	848	13.2	1.251	0.207
	DD	430	830	12.5	1.223	0.206
	TD	420	821	12.1	1.212	0.205

## Quasi-static Nakajima Test

## 2.1. Test procedure

The test rigs for quasi-static Nakajima test are shown in Fig. 3. The diameter hemispherical punch is 10mm. To obtain the various strain ratios of the deformed specimen, different specimen geometries with widths of middle section of 10mm, 20mm, 30mm and 40mm are used as shown in Fig. 5. Here, the strain ratios of the deformed patterns range between the simple tension region to the biaxial stretch region. The width of 40mm specimen is used to obtain biaxial tension mode and The width of 30mm specimen is used to obtain stretching mode. Plane strain mode is obtained from the width of 20mm specimen size and uniaxial tension mode is obtained from the width of 10mm specimen size. The rigs are performed on the MTS to record the punching speed and the punching force as shown in Fig. 4. Lubrication condition with lubricating grease is applied between the specimen and the punch.

## 2.2. FLC test result

The forming limit diagram(FLD) is providing a graphical description to the maximum deformation a material can withstand prior to failure. Within the FLD the forming limit curve(FLC) depicts the maximum deformation to failure for different states of in-plane strains, where  $\epsilon_1$  is the major strain and  $\epsilon_2$  is the minor strain. The strain can be obtained from grids marked on the surface of the specimen. The circle grids(each diameter is 100 $\mu$ m)are printed by Photolithography method as shown in Fig.6(1), which become elliptical during deformation. The deformed grids in the first row next to fracture curve are considered as necking and the grids in the second row are safe. The deformation of grids near the fracture is measured with a microscope so that the major strain and the minor strain could be determined as shown in Fig.6(2).

Figure 7 shows fractured specimens after testing at quasi-static Nakajima test. The localized fracture of the specimens took place in the center of the specimen which indicates a lower sensitivity to the friction conditions. The schematic diagrams of each specimen for the quasi-static test are used to construct the FLC as shown in Fig. 8. The forming limits are the result of maximum of interpolated bell-shaped curves. For the tested thin sheet metal, no complete shift up or downwards of the FLC.

## High Speed Nakajima Test

### 3.1. Test procedure

A high speed crash testing device is designed to evaluate the forming limit of the ultra-thin sheet metals. As shown in Fig. 9, the device has six parts: compressed air bottle, pressure regulator, pressure storage, pressure check valve, Cylinder and punching jigs. The Nakajima test parameters in high speed test are same as quasi-static test. Maximum air pressure in pressure storage is adjustable from 0.8Mpa to 5.0Mpa under the pressure regulator. The schematic design of high speed punching device is shown in Fig. 10. The punch can be accelerated by the pneumatic system at maximum velocities up to 20m/s. As

shown in Fig. 11, high speed camera is mounted in front of the forming device. The camera records the velocities of punch with frequencies up to 2000Hz.

In contrast to the quasi-static Nakajima test, the high speed Nakajima test cannot stopped precisely at the onset of a fracture in a specimen because the punch speed is too fast for the fracture moment. A lot of dry runs are carried out to find the optimal dome height by adjusting the distance between the support frame and the forming device. The fracture moment is obtained by regulating the distance through repeat experiment.

### **3.2. Experimental result**

The fracture depth is abstained from the high-speed Nakajima test as shown in Tab.3. The fracture depth with punch speed at 12m/s for ultra-thin sheet metal with thickness of 30 $\mu$ m is about 2mm, thickness of 60 $\mu$ m is about 3mm, thickness of 100 $\mu$ m is about 4mm. However, The fracture depth for specimen in quasi-static Nakajima test at 0.08mm/s punch speed with thickness of 30 $\mu$ m is about 3mm, thickness of 60 $\mu$ m is about 5mm, thickness of 100mm is about 7mm. Obviously the fracture depth in high-speed Nakajima test decreases comparing with the quasi-static Nakajima test result for both cases shown as Tab.3. The specimens with thickness of 30 $\mu$ m shows the lowest fracture depth value in both high-speed Nakajima test and quasi-static Nakajima test. Fig. 12 shows fractured specimens after testing at high speed Nakajima test. The fracture of the specimens mainly takes place near the center of the specimen, which is different with the quasi-static Nakajima test result. It indicates the specimen under high speed punch is more sensitive to the friction conditions.

Tab.3 Fracture depth

Thickness( $\mu\text{m}$ )	Loading direction	Fracture depth(mm)	
		Quastic test	High-speed test
30	10	3.3	2.5
	20	3.2	2.3
	30	3.1	2.2
	40	3	2
60	10	5.4	3.4
	20	5.2	3.3
	30	5.2	3.1
	40	5	3
100	10	7.2	4.2
	20	7.1	4.1
	30	7.1	4
	40	7	3.9

Based on the speed measurements, the strain rates are estimated by dividing the evaluated major strains by time needed for a full stroke. The mean strain strain rates for quasi-static test with punch speed at 0.08mm/s is 0.0027s<sup>-1</sup> and for high-speed test speed at 12m/s is 2.4×10<sup>3</sup>s<sup>-1</sup>. Forming limit curves comparison at 12m/s punch speed and 0.08mm/s punch speed is shown in Fig. 13. There is a distinct difference in the strain states between specimens tested at quasi-static test and at high-speed test. Punching speed drastically affects the formability of the test metal. The high speed punching leads to a lower FLC both in the right side of biaxial stretching and the left side of uniaxial stretching. The averaged decrease in major strain ranged from 20–30% for tension area, and from 30–50% in the plane strain regime. In all the cases, the forming limit curves shift downward is observed in all cases of the specimen with different thickness. Both sides of FLC for all cases specimen at high speeds is shorter than the quasi-static curves. However, the left side of FLC for 30 $\mu\text{m}$  thickness specimen at high speed goes close to the FLC at quasi static speed. The reason for this phenomenon might be the increase of uniform elongation during dynamic deformation. However, the right hand side of FLC at high speed goes lower than that at quasi static speed.

The specimen for thickness of 100 $\mu\text{m}$  at high speed forming shows higher strain range than the other ones. The result is similar with the quasi static test. The result implies the higher thickness specimen with more grains across the section have better formability both in high speed forming and quasi static forming .

### 3.3. Result discussion

From the macro level to describe the deforming process, sheet metal forming involves large plastic strains that may induce ductile damage, concluding initiation, growth and coalescence of microvoids and microcracks and degradation of material properties[13]. The deformation behavior and fracture depend on the mechanism for the deformation twinning and dislocation slip. In macro level similar result is obtained that the high-speed FLCs are lower than the static FLCs in the biaxial stretch region due to the shear fracture[5]. The shear fracture decreases the ductility of sheet metals. Study also shows that fracture mode is mainly caused by ductile fracture at high strain rate[12]. As strain rate increases, the twin density will increase significantly. This is mainly because the flow stress increases dramatically with the increasing of strain rate and higher flow stress makes it easier for twinning to nucleate and evolve. Then transformation from mixed fracture mode of ductile fracture and cleavage fracture to thorough ductile fracture when tensile strain rate increases from quasi-static to very high strain rate.

Previous arts reported that the tooling-workpiece interfacial friction increases with the decrease of specimen size[14]. This size effect can be explained by the increase of the proportion of real contact area while interfacial friction will decrease with the increase of grain size due to the decrease of grain boundary strengthening effect and the increase of surface grain fraction. The localized fracture of specimens for the quasi-static test took place in the center of the specimen which is lower sensitivity to the friction conditions comparing with the fracture near the center of the specimen for high speed test. It indicates the interfacial friction in high speed test is more sensitive comparing with the quasi-static case.

For this study when the specimen thickness get to the micron level, there are several grains across the thickness. The number of grains would be small and each grain's crystallographic property would play crucial role in the plastic behavior of the material. The surface grain and inner grains play different roles in the slipping-twinning transition. Especially the deforming process varies with high strain rate in high speed deformation. So This should give impetus to further work on exploring how the forming speed affect the formability in micro level.

## Conclusion

With this paper, high speed Nakajima tests and quasi-static Nakajima tests with the ultra-thin 304 sheet metal have been presented. The developed high-speed Nakajima testing device and quasi-static testing device has developed for the deformation at high speed and quasi-static forming. The punching speed is recorded by high-speed camera. The defining FLC under different strain rate is illustrated by measuring deformation of grids near the fracture.

(1) The results of tensile test are used to evaluate the formability of 304 ultra-thin metal sheet at quasi static test speed. The tension character is significantly related to the micro structure of specimens. The specimen with higher thickness shows higher hardening coefficient and elongation than the thinner ones. This result implies the higher thickness specimen with more grains across the section have better formability.

(2) Forming speed drastically affects the formability of the test metal. The presented high-speed FLC(at 10m/s punch speed) both in the right side and the left side is lower than quasi-static speed FLC(at 0.08mm/s punch speed) for 304 ultra-thin metal sheet with thickness 0.01mm, 0.03mm, 0.1mm. Both sides of FLC for all cases specimen at high speeds is shorter than the quasi-static curves. The left side of FLC for thinner specimen at high speed goes close to the FLC at quasi static speed. However, the right hand side of FLC at high speed goes lower away than that at quasi static speed.

## Declarations

### Availability of data and material

Data is available.

### Competing interests

The authors declare no competing interests.

### Funding

PhD Foundation of Shandong Jianzhu University.

### Authors' contributions

ZY developed the main study ideas. ZY wrote the main part of the manuscript and took part in the planning and execution of the fermentation experiments. XCY, YZJ and TXJ also wrote parts of the manuscript and carried out the main part of the experiments, analyzed the results. ZGQ reviewed the manuscript. All authors read and approved the final manuscript.

### Acknowledgements

The authors would like to thank Shandong Jianzhu University for providing necessary financial assistance.

## References

1. Clark D S. The tensile impact properties of some metals and alloys[J]. Trans. ASM, 1950, 42–45.
2. Balanethiram, V.S., Daehn, G.S., 1992. Enhanced formability of interstitial free iron at high strain rates. Scripta Metallurgica et Materialia 27, 1783–1788.
3. Balanethiram, V.S., Daehn, G.S., 1994. Hyperplasticity: Increased forming limits at high work piece velocity. Scripta Metallurgica et Materialia 30, 515–520.
4. Hu, X.H., Wu, P.D., Lloyd, D.J., Embury, J.D., 2014. Enhanced formability in sheet metals produced by cladding a high strain-rate sensitive layer. Journal of Applied Mechanics 81.

5. Kim S B, Huh H, Bok H H, et al. Forming limit diagram of auto-body steel sheets for high-speed sheet metal forming[J]. *Journal of Materials Processing Technology*, 2011, 211(5): 851–862.
6. Kiliçlar Y, Demir O K, Engelhardt M, et al. Experimental and numerical investigation of increased formability in combined quasi-static and high-speed forming processes[J]. *Journal of Materials Processing Technology*, 2016, 237: 254–269.
7. Taebi F, Demir O K, Stiemer M, et al. Dynamic forming limits and numerical optimization of combined quasi-static and impulse metal forming[J]. *Computational Materials Science*, 2012, 54: 293–302.
8. Fu M W, Chan W L. A review on the state-of-the-art microforming technologies[J]. *The International Journal of Advanced Manufacturing Technology*, 2013, 67(9-12): 2411–2437.
9. Gronostajski Z, Pater Z, Madej L, et al. Recent development trends in metal forming[J]. *Archives of Civil and Mechanical Engineering*, 2019, 19(3): 898–941.
10. Xu J, Wang X, Wang C, et al. A review on micro/nanoforming to fabricate 3D metallic structures[J]. *Advanced Materials*, 2021, 33(6): 2000893.
11. Malik A, Yangwei W, Huanwu C, et al. Fracture behavior of twin induced ultra-fine grained ZK61 magnesium alloy under high strain rate compression[J]. *Journal of Materials Research and Technology*, 2019, 8(4): 3475–3486.
12. Zhu C, Xu J, Yu H, et al. Size effect on the high strain rate micro/meso-tensile behaviors of pure titanium foil[J]. *Journal of Materials Research and Technology*, 2021, 11: 2146–2159.
13. Korhonen, A.S., Manninen, T., 2008. Forming and fracture limits of austenitic stainless steel sheets. *Mater. Sci. Eng. A* 488, 157–166.
14. Engel U. Tribology in microforming[J]. *Wear*, 2006, 260(3): 265–273.

## Figures

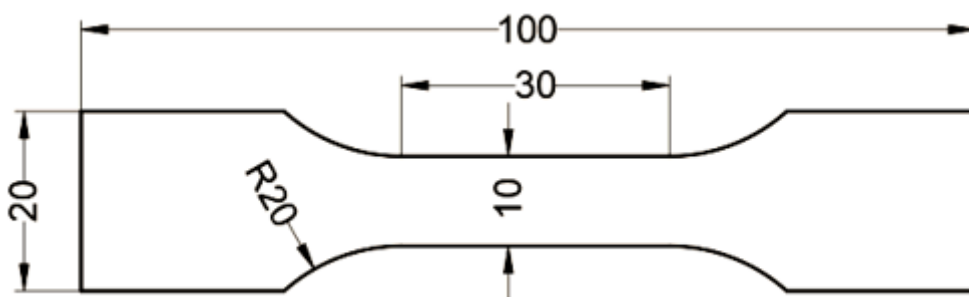
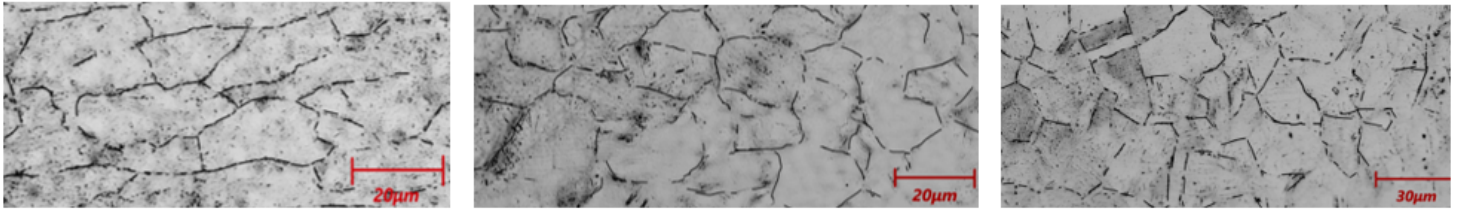


Figure 1

Testing specimen



(1) 30μm

(2) 60μm

(3) 100μm

**Figure 2**

Microstructures of the material through the thickness section

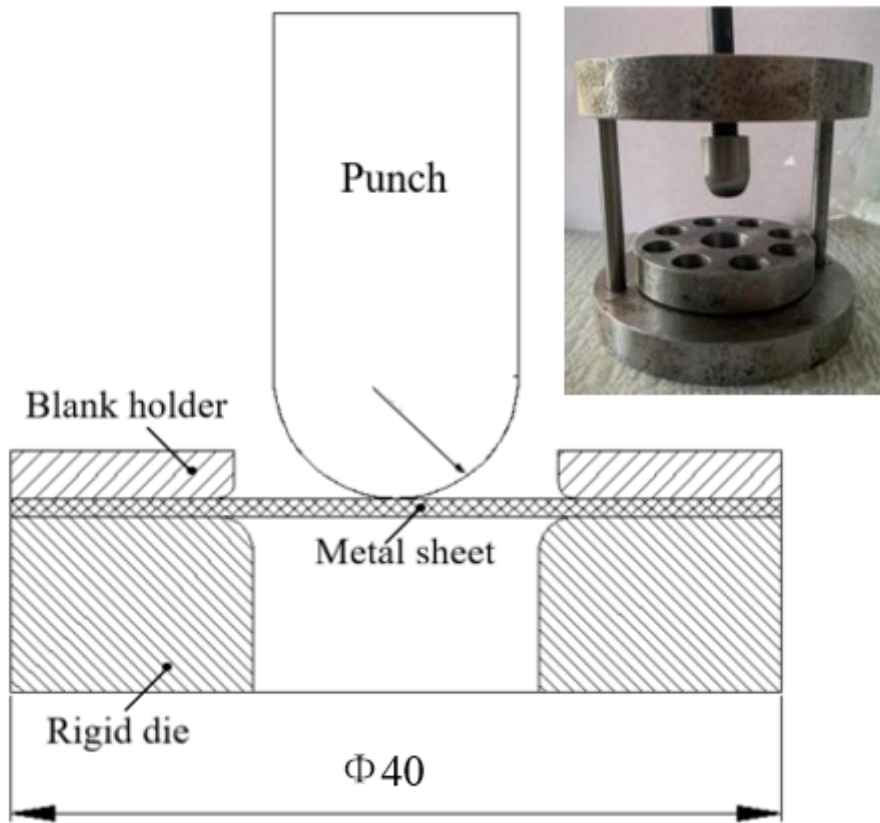


**Figure 3**

Sketch of Punching rigs for the quasi-static test



Figure 4

The quasi-static test setup

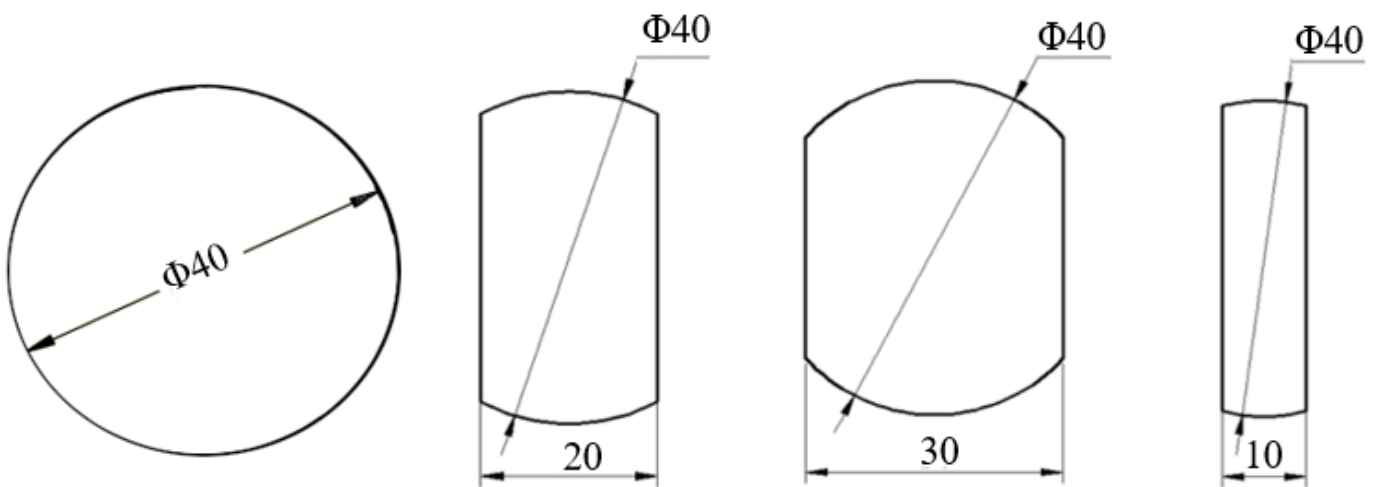
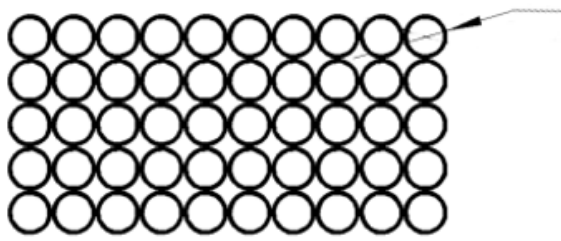


Figure 5

Geometry of tested specimens



( 1 ) Circle grids printed on the surface of the tensile specimen

( 2 ) Grids testing

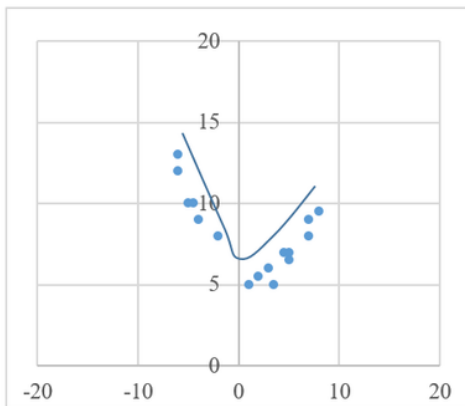
Figure 6

Grids and testing

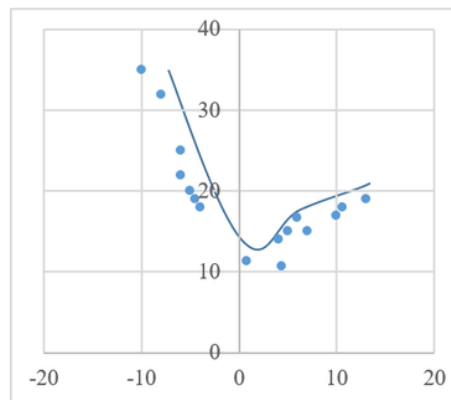


Figure 7

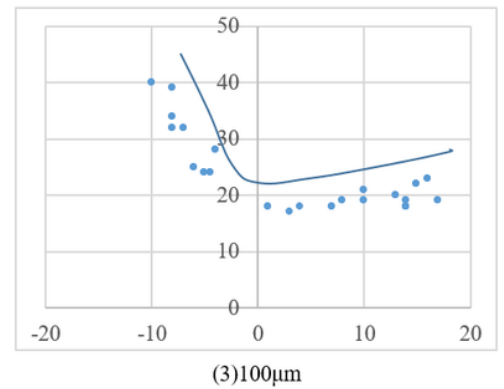
Fracture specimens for quasi-static test



( 1 ) 30µm



(2) 60µm



(3)100µm

Figure 8

Forming limit curve for quasi-static test

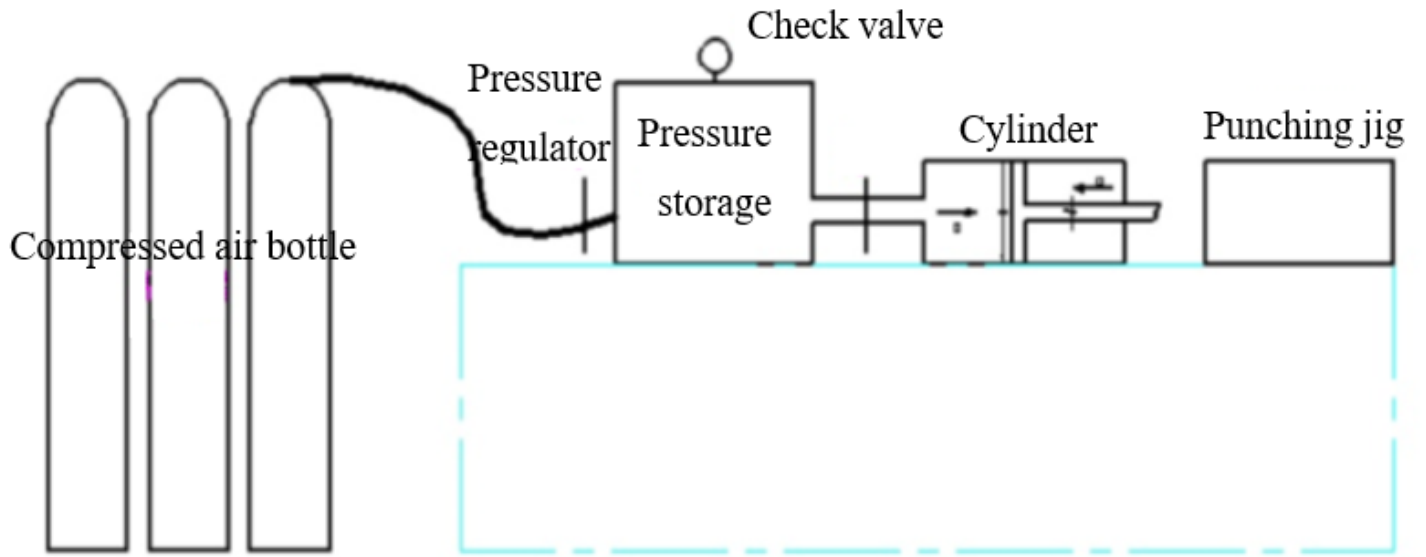


Figure 9

Schematic design of high speed crash testing device design

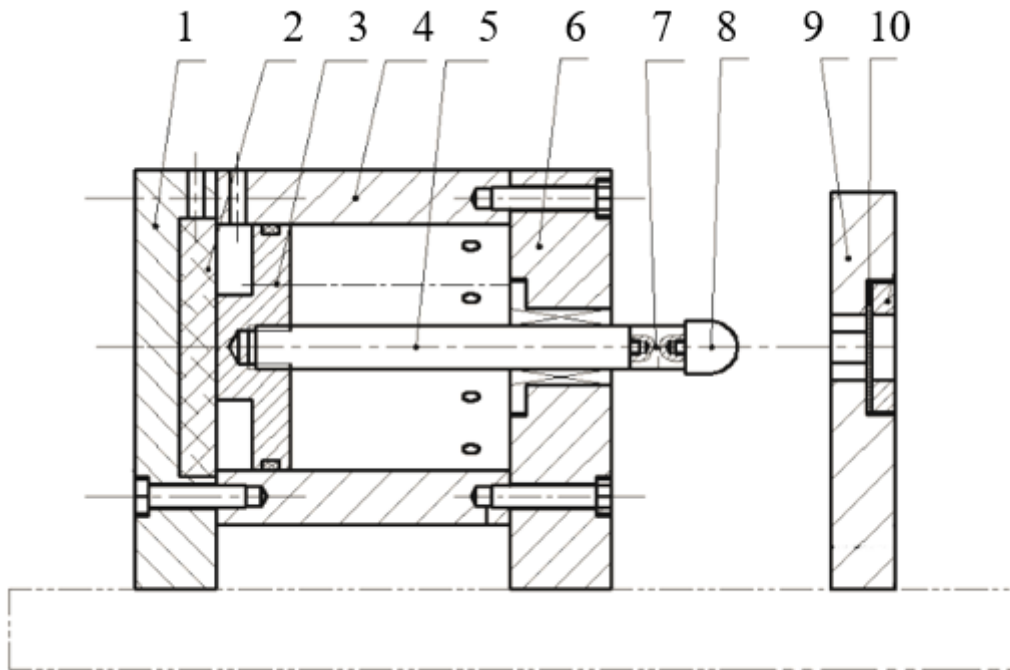
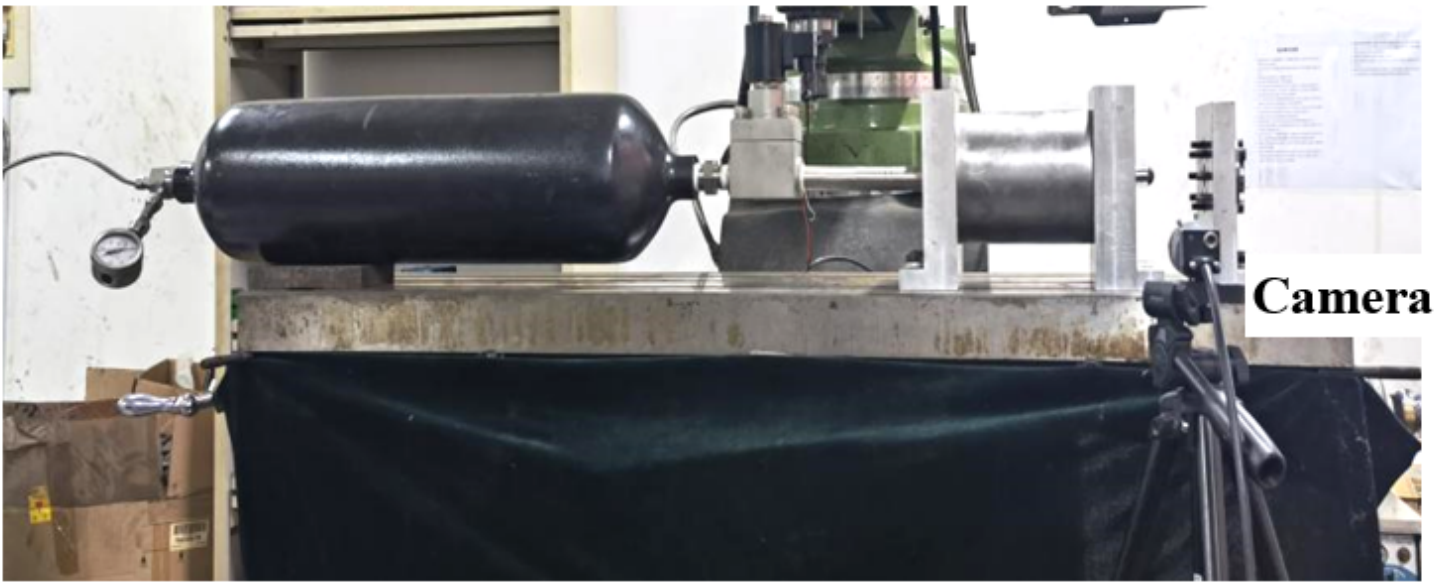


Figure 10

Schematic design of high speed punching device

1. Cover 2. Magnet 3. Piston 4. Cylinder barrel 5. Piston rod 6. Cover 7. Connecting bolt 8. Punch 9. Support frame 10. Specimen



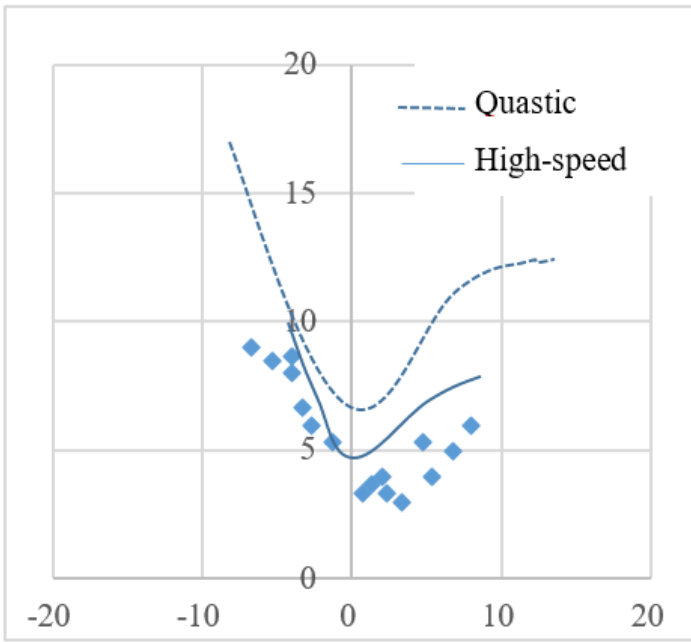
**Figure 11**

High speed crash testing device

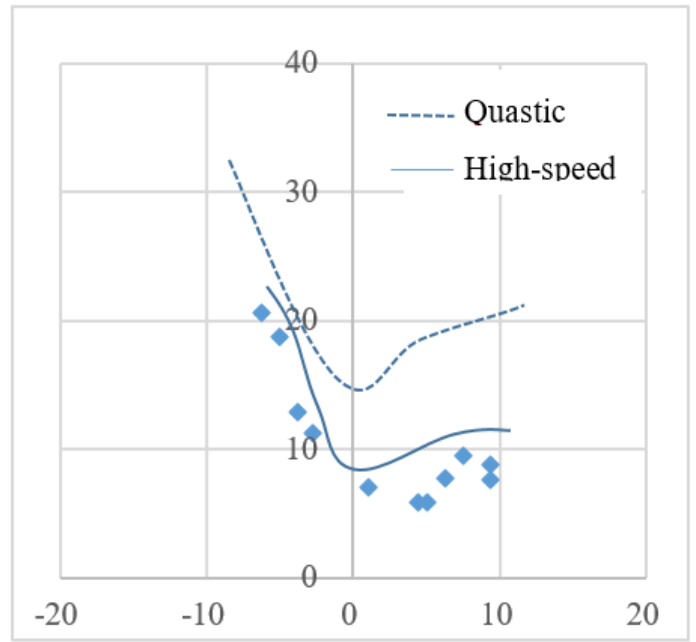


**Figure 12**

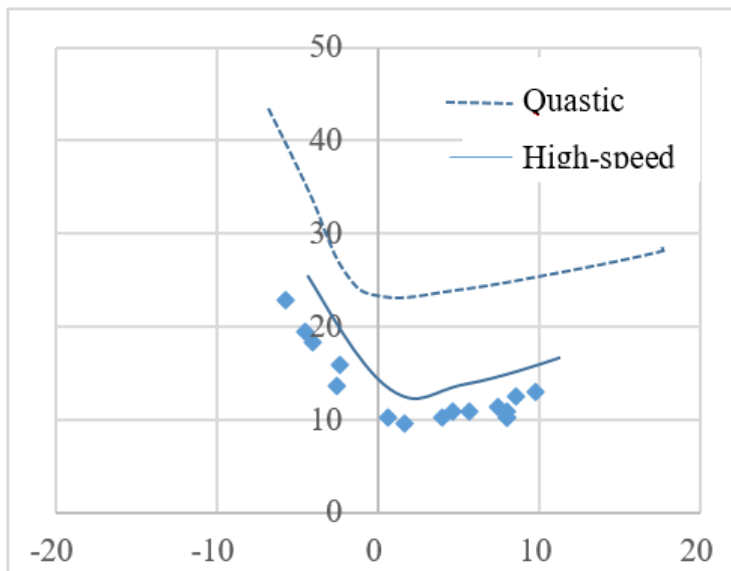
Fracture specimens for high speed test



( 1 ) 30 $\mu$ m



( 2 ) 60 $\mu$ m



( 3 ) 100 $\mu$ m

**Figure 13**

Forming limit curves for high-speed test